

Multi-criteria GA-based Pareto optimization of building direction for rapid prototyping

Ye Li · Jian Zhang

Received: 29 January 2013 / Accepted: 19 June 2013 / Published online: 7 July 2013
© Springer-Verlag London 2013

Abstract Selection of a building direction is an important step for rapid prototyping regardless of the specific processes used to create the part. It involves the consideration of multi-factors that have influences on surface quality, build efficiency and support structure, etc. Contemporary approaches did not consider the global directional space to search for the optimal building direction. In this paper, we use a multi-sphere model for multi-criteria optimization of building direction in rapid prototyping. Each sphere represents the global directional space for one optimization criterion, and is obtained by uniformly discretizing the surface of a unit sphere. Optimization is then conducted over each discretized spherical surface for each criterion. Two objectives, *theoretical volume deviation* (TVD) and part height are simultaneously optimized using genetic algorithm. TVD is computed to evaluate the volumetric error along each building direction in a general way. The Pareto front is computed as well in order to study the competing effect from these two criteria. At the end of the paper, examples are presented to show the effectiveness of the method.

Keywords Rapid prototyping · Building direction · Volume deviation · Pareto optimization · Genetic algorithm

1 Introduction

Rapid prototyping is a group of additive manufacturing processes that construct physical objects through building and stacking layers [1]. Regardless of the specific processes used

to create layers, each layer is stacked on the previously created layer sequentially along a building direction according to the CAD (computer-aided design) information. The selection of a building direction has impacts to surface quality, build height, support structure, building efficiency, material strength, etc. This has made the selection of building direction an important process planning step for rapid prototyping.

In order to find the optimal building direction, different criteria have been used. One widely considered criterion is part surface quality, resulting from the staircase effect inherent to all rapid prototyping processes. Byun and Lee [2] used arithmetic mean surface roughness to evaluate surface quality. The concept of surface roughness was adapted to rapid prototyping processes with layer thickness, layer fillet, and corner radius incorporated when calculating surface roughness. Ahn et al. [3] studied the relation of surface roughness with layer thickness, surface angle, and surface profile angle. Giannatsis and Dedoussis [4] used regression analysis to predict surface roughness for the stereolithography system based on example part measurements. Canellidis et al. [5] and Nikhil and Kalyanmoy [6] considered both up faces and down faces along the building direction to evaluate surface roughness. In addition to surface roughness, volumetric error is also used to describe the deviation between the solid model and the part produced with staircases. Rattanawong et al. [7] analyzed volumetric error of basic primitive geometries, and treated more complex parts as combinations of primitive geometries. Masood and Rattanawong [8] calculated the volumetric error at each layer using sliced polygonal contours of each layer and the layer thickness. Kumar and Choudhury [9] presented a method of calculating the volumetric deviation between a CAD model and the part made by five-axis laminated object manufacturing. Recently, Zhang and Li [10] used a heuristic rule to map volumetric deviation information onto a discretized unit sphere and search for the optimal building direction on the discretized unit spherical surface.

Y. Li (✉)
Department of Industrial and Manufacturing Engineering and
Technology, Bradley University, Peoria, IL 61625, USA
e-mail: yli@bumail.bradley.edu

J. Zhang
Microsoft Corporation, Redmond, WA 98052, USA
e-mail: fdujian@hotmail.com

Similar to any production machinery, a rapid prototyping machine also has a limited range for producing parts. If a part model does not fit into the dimensional ranges, then the part is not producible on that machine. For rapid prototyping processes, build height is an index used to evaluate the manufacturability of a model on a particular rapid prototyping machine. Moreover, build height is also relevant to build time [11–13]. Chan and Tan [14] developed an algorithm to test if a 3D model will fit within a cylindrical volume. The algorithm can be used to search for the building direction since both the minimum diameter cylinder and the minimum height cylinder can be determined. Optimizing build height is particularly important when packing multiple parts in one setup on a rapid prototyping machine [11, 12], where the objective is to maximize the space utilization. Other criteria considered in choosing building direction include support structure, mechanical properties, trapped volumes, etc. Allen and Dutta [15] considered support structure in optimizing building direction. The direction that leads to a lower center of mass is preferred in their algorithm. Thompson and Crawford [16] used the criterion of mechanical property. Kim et al. [17] calculated the trapped volume along the building direction.

Since the building direction has impacts to many aspects on parts made from rapid prototyping processes, many researchers have taken multi-objective optimization approaches to identifying the optimal building direction. Cheng et al. [18] summarized the general attributes of an optimal building direction and presented a framework that optimizes each criterion sequentially. Hur et al. [11] optimized the building direction and packing problem for selective laser sintering (SLS) process with the objectives on part height, build time, and surface quality. The orientation and packing optimization employed a modified bottom-left approach and was implemented in genetic algorithm (GA). Byun and Lee [2] considered surface roughness, build time, and part cost in their optimization, and the optimal direction for each criterion is identified. Candidate directions in their research are generated from the convex hull of the part model. Hur and Lee [19] determined the optimal building direction that has better part accuracy, shorter build time, and less support structure for StereoLithography (SLA) process. A user can choose the rank for these three criteria in the optimization process. Canellidis et al. [5] used a multi-criteria genetic algorithm to optimize build time, surface roughness, and post-processing time for SLA process. The objective function took a weighted approach to incorporate different criteria.

In order to study the trade-off between competing factors during optimization, the concept of Pareto front is applied in multi-criteria optimization. Pandey et al. [20] optimized average surface roughness and build time at the same time for fused deposition modeling process using GA. Adaptive slicing is implemented so that surface roughness is maintained below a specific level, and Pareto front is computed for surface

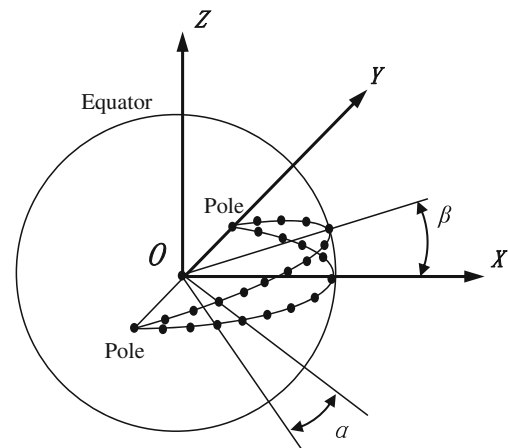


Fig. 1 Discretization of a unit sphere with two fixed rotational angles [38]

roughness and production time. Ancau and Caizar [13] computed the Pareto front of surface roughness and manufacturing cost. Recently a bi-objective optimization using both multi-objective genetic algorithm and particle swarm optimization was presented by Nikhil and Kalyanmoy [6] to optimize surface roughness and build time of SLS process. Trade-off between these two factors was studied with an approximate Pareto front.

Determining the optimal building direction in rapid prototyping processes generally involves the stages of generating candidate directions, selecting criteria, evaluating candidate directions, and ranking candidate directions with competing criteria. Previous studies chose candidate directions by convex hull [2], feature analysis [4], rotating along coordinate axes by fixed angles [8, 13]. These methods are not able to massively and accurately explore the directional space. Recently, Zhang and Li [10] applied Saff and Kuijlaars' discretization method [21] to uniformly sample a unit sphere. The purpose is to provide a global space that

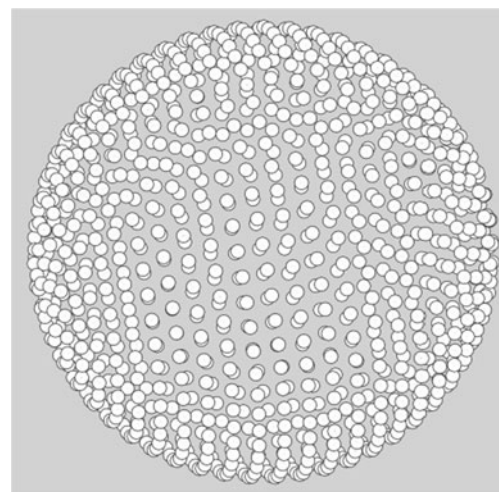
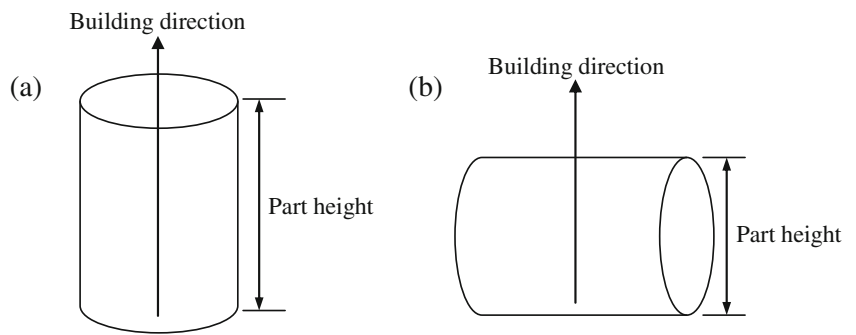


Fig. 2 Ten thousand points sampled from a unit sphere [10]

Fig. 3 Impact of building direction on different criteria



maximally represents potential directions in a 3D space. As most prototypes are used to evaluate geometric form and function, almost all the previous researchers have the criterion of surface quality in their optimizations. Although surface roughness can be used to evaluate surface quality, its calculation is dependent on the specific rapid prototyping process. In this paper, Saff and Kuijlaars’ algorithm [21] is applied to generate the global directional space by massively and accurately sampling a unit sphere surface; *theoretical volume deviation* (TVD) is proposed to give a general way to calculate the volume deviation between a tessellated model and the actual built volume; part build height is also calculated along each candidate direction as a secondary optimization criterion and is optimized simultaneously with theoretical volume deviation; Pareto front is computed in order to handle these two competing criteria. The multi-criteria optimization is implemented with genetic algorithm which is

able to explore the entire search space stochastically and extensively

2 Method

2.1 Global directional space discretization

Global direction space is the collection of all directions in a 3D space, and this space has been described geometrically as a unit sphere. A unit sphere is a sphere with unity radius, which is formed by moving all normalized 3D direction vectors to a same starting point, the center of the unit sphere. The concept of unit sphere has been applied to study CNC machining setup [22] die and mold design [23] and CMM inspection planning [24]. For rapid prototyping, there are an infinite number of potential building directions with respect

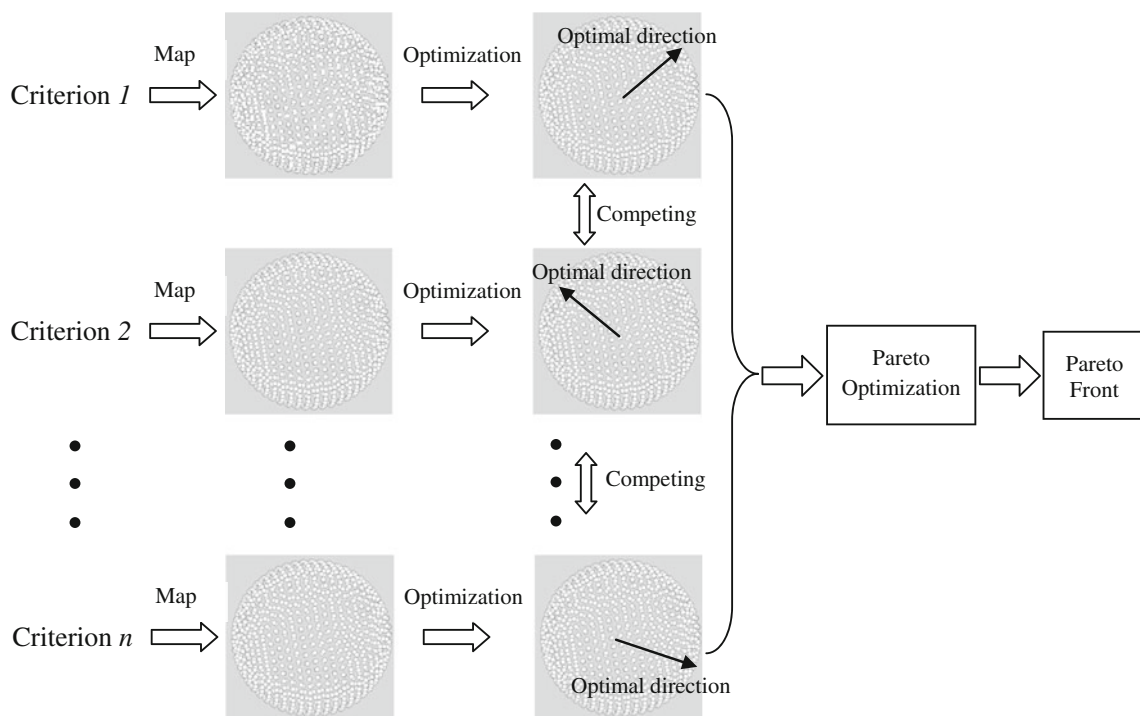


Fig. 4 Multi-objective optimization of RP building direction

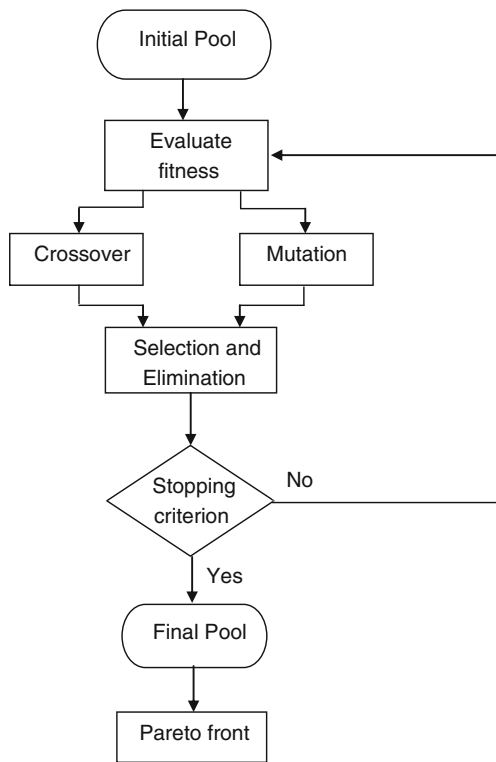


Fig. 5 GA-based Pareto optimization

to the machine coordinate system. Similarly, all those potential building directions collectively form a unit sphere.

In order to find the optimal building direction, a search will be conducted on the unit sphere that carries all potential directions. Although a spherical surface is continuous and differential, many researchers used discretization approach to study the problems on a unit sphere in order to avoid numerical complexity. Generally, there are two ways of discretizing a unit sphere. One is triangle-based discretization where a unit sphere surface is partitioned into triangles or spherical patches; the other is point-based discretization that discretizes a unit spherical surface with a grid of points. Yang et al. [25] obtained discretized points on a unit sphere through triangulation to

check tool accessibility. Dhaliwal et al. [26] triangulated the spherical surface of a unit sphere with fixed resolution to calculate visibility. Although spherical surface triangulation is able to partition a unit sphere surface with controlled resolution, the shape of tessellation triangles is hard to maintain uniform. Therefore the discretization is not uniform on the spherical surface.

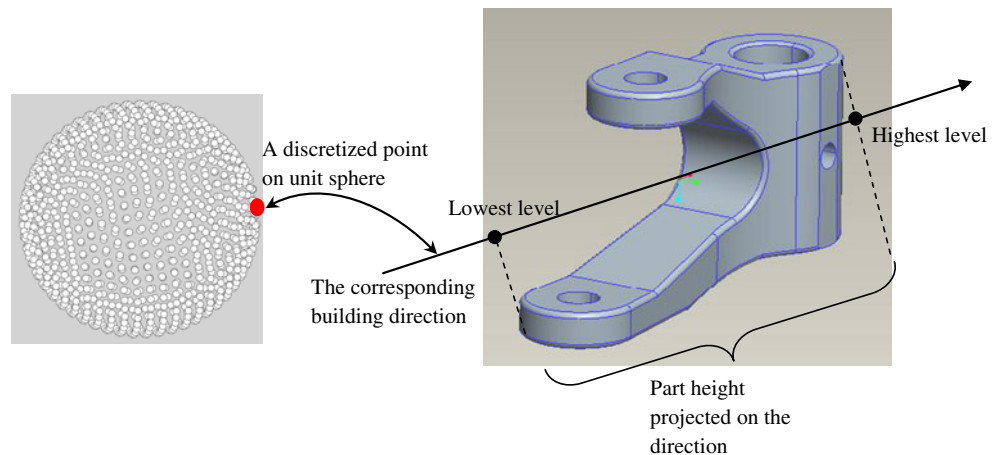
Point-based discretization breaks a unit sphere into an array of spherical points and the computation on a unit sphere becomes operations on the grid of points. Most point-based discretization used in manufacturing process planning used two fixed rotational angles [8, 13, 38]. Figure 1 shows an example with the two fixed rotational angles. It can be seen that the points are distributed relatively sparse near the equator while gradually becoming closer when moving towards the two poles. Therefore, it is not a uniform discretization of a unit sphere either.

In order to create a uniformly sampled global directional space for rapid prototyping processes, Zhang and Li [10] adopted Saff and Kuijlaars' spiral points construction algorithm [21] to distribute points evenly on a unit sphere. Volumetric error information is then mapped onto this space using a heuristic rule, followed by an optimization procedure to identify the optimal building direction. Saff and Kuijlaars' algorithm [21] has been shown to be effective in discretizing unit sphere surface, particularly when the number of discretization points N is large. In this paper, we intend to optimize two criteria simultaneously for the building direction of rapid prototyping processes. Saff and Kuijlaars' algorithm [21] is applied to generate the global directional space for each optimization objective. Figure 2 shows the generated spiral points on a unit sphere when the number of points $N=10,000$.

2.2 Multi-sphere optimization model

Optimization of building direction for rapid prototyping processes involves many factors; as one objective is being

Fig. 6 Part height calculation



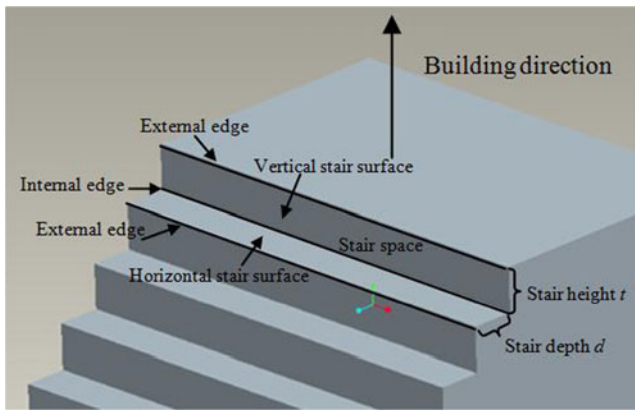


Fig. 7 Parameters of a stair

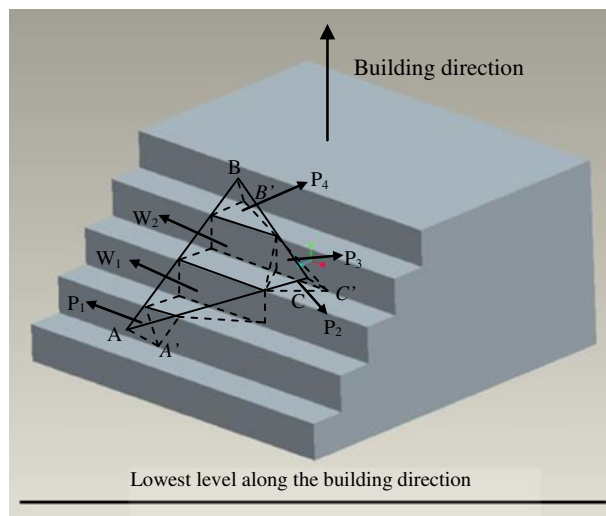
optimized, other objectives may be compromised at the same time. The nature of finding optimal building direction is a multi-objective optimization process. This can be illustrated in Fig. 3, where a cylinder is to be produced by rapid prototyping processes. This example takes two intuitive building directions as shown in Fig. 3a, b. In Fig. 3a, the building direction renders good surface quality since the triangular facets are either parallel or perpendicular to the building direction; so the volume deviation is minimized. However, the part height in Fig. 3a is higher than that in Fig. 3b, suggesting a longer build time. The building direction in Fig. 3b requires minimal part height on the machine, but the volume deviation on the cylindrical surface is more significant compared with that in Fig. 3a. Two factors, volume deviation and part height, are competing against each other as the building direction is varying.

In order to find the optimal building direction, a part height H_i and volume deviation V_i can be calculated for every building direction $D(\theta_i, \phi_i)$ on a unit sphere. Traditional optimization algorithm will combine the two criteria into a single one W by aggregating two parameters V and H with their weights w_1 and w_2 into $W = w_1H + w_2V$. In this way, a multi-objective

optimization is transformed into a single-objective optimization, and the algorithms developed for single-objective optimization can be directly applied to search through the optimization space to optimize the single criterion W . This method has been widely used in many cases where multi-objective optimization problems are simplified into a single-objective one. In spite of its simplicity, there are often no clear rules on how to rank the relative significance of each individual optimization criteria; the final result is therefore subject to user’s choice of weights w_1 and w_2 . For multi-objectives that are competing against each other, it is very hard to find a single solution that simultaneously optimizes each objective. Usually when one objective is improved, the others will be compromised. In order to deal with such a scenario, a set of optimal solutions, called *Pareto front*, can be computed in which none of them can be eliminated without worsening one of the objectives [27–30].

The example presented in Fig. 3 is a simple geometric model, and one can intuitively select the building direction by considering the relative importance of those two factors. As rapid prototyping has been considerably used to make complicated geometries and even free-form surfaces, there is a need for developing a general model that can be used to assist users in selecting the optimal building direction. Figure 4 shows a multi-sphere optimization model based on Pareto optimization. The input information consists of multi-criteria in rapid prototyping processes. The information of each criterion is then mapped onto a discretized unit sphere, followed by an optimization on each discretized unit sphere. As there are multi-criteria in the optimization, there are a plural of discretized unit spheres, collectively representing the complete global optimization space. The optimization is conducted on each discretized unit sphere initially; then the result on each unit sphere goes to the Pareto optimization unit in Fig. 4. The output of Pareto optimization unit is a Pareto front that is presented to the user for decision-making. A number of

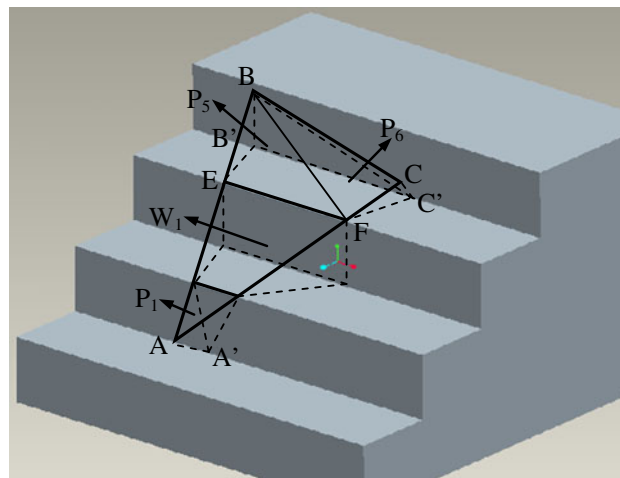
Fig. 8 Three vertices in three different stair spaces



- P₁: Pyramid Type 1
- P₂: Pyramid Type 2
- P₃: Pyramid Type 3
- P₄: Pyramid Type 4
- W₁: Wedge Type 1
- W₂: Wedge Type 2

A', B' and C' are the projections of A, B, and C on internal edges

Fig. 9 Two vertices in one stair space with the third vertex in a different stair space



P_1 : Pyramid Type 1
 P_5 : Pyramid Type 5
 P_6 : Pyramid Type 6
 W_1 : Wedge Type 1
 A' , B' and C' are the projections of A , B , and C on internal edges

multi-objective evolutionary algorithms have been proposed to solve the multi-objective optimization problems. Most of them use non-dominant ranking and selection to evolve the solution towards the Pareto front. In this paper, a Pareto GA algorithm is developed to search for the set of building directions that constitute the Pareto front of solutions.

2.3 GA-based Pareto optimization

GA is a stochastic optimization method that mimics natural evolution, whereby individuals in each generation go through the processes of crossover, mutation, and selection [31–34]. As a randomly guided searching technique simulating the evolutionary process in nature, GA is able to navigate through huge search spaces to look for optimal solutions intelligently. As is shown in Section 2.1 that the candidate building direction space on the unit sphere is large, a genetic algorithm is then used in this research to stochastically search through the candidate building direction space to increase the searching efficiency. Since multi-factors are involved in determining the globally optimal building direction for RP processes, we use an evolutionary multi-objective optimization, instead of having

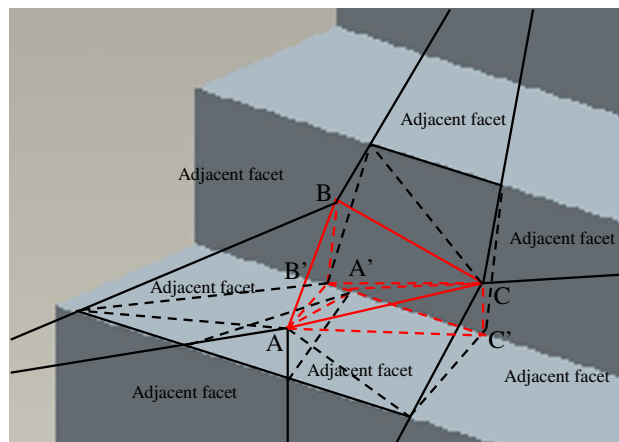
a single objective criterion. It is not unusual that different optimization objectives are competing with one another in multi-objective optimization [35, 36]; therefore, a Pareto genetic algorithm is developed to solve the multi-objective optimization problem in the presence of trade-offs between competing objectives [27–30]. In this research, two factors, volume deviation and part height, are considered. This section will illustrate the design of the GA-based Pareto optimization.

In this research, the Pareto front is the set of solutions $(H_1, V_1), (H_2, V_2), \dots, (H_k, V_k)$ that for each $i \in (1, k)$ we cannot find any other solution (H_m, V_m) that satisfies both $H_m < H_i$ and $V_m < V_i$. The detailed GA-based Pareto algorithm design is explained as follows (Fig. 5):

Step 1: initial population generation N_p initial building directions $(D_i(\theta_i, \phi_i), i \in (1, N_p))$ are randomly selected from all the discretized directions on the unit sphere to form an initial pool of first generation solutions with the size of N_p .

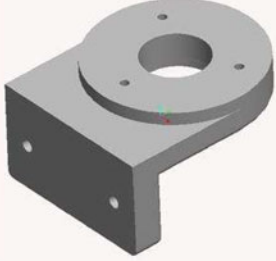
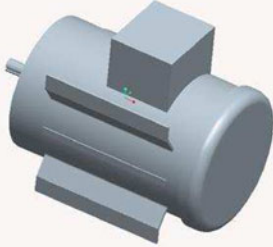
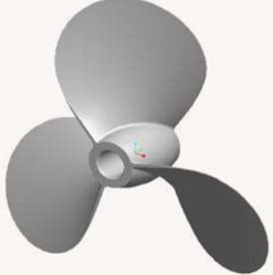
Step 2: fitness criteria For every candidate directions in the pool, we calculate both the part height and volume deviation (H_i, V_i) for each direction $D_i(\theta_i, \phi_i), i \in (1, N_p)$.

Fig. 10 Three vertices in one stair space



Pyramid $B'-ABC$: Pyramid Type 7 (P_7)
 Pyramid $A'-AB'C$: Pyramid Type 8 (P_8)
 Pyramid $C'-CAA'$: Pyramid Type 9 (P_9)
 A' , B' and C' are the projections of A , B , and C on internal edges

Table 1 Three example part models

Part Number and Name	1. Motor mount	2. Motor	3. Bladed propeller
Part Geometry			
Number of Facets	880	840	1052

Step 3: crossover and mutation Within each generation, p percent of the new solutions will be generated by crossover and $(1-p)$ percent of the new solutions will be generated by mutation. To get an offspring solution by crossover, two parent solutions (θ_i, ϕ_i) and (θ_j, ϕ_j) are randomly picked up from the solution pool and the new solution $(\theta_{\lfloor \frac{1}{2}(i+j) \rfloor}, \phi_{\lfloor \frac{1}{2}(i+j) \rfloor})$ is generated through mating actions on index i and j ($\lfloor \cdot \rfloor$ is the rounding operator). To get an offspring solution by mutation, a building direction (θ_n, ϕ_n) is randomly chosen from the discretized points on the unit sphere and is added into the generation pool. Totally N_e new solutions will be generated so that the next generation pool will have $N_p + N_e$ solution building directions.

Step 4: selection and elimination The goal of this step is to decrease the number of solutions in the pool from $N_p + N_e$ back to N_p . Non-dominant objective solutions are removed from the pool. A non-dominant objective solution is the set

of (H_i, V_i) that has at least another solution (H_j, V_j) in the pool that satisfies $H_i \geq H_j$ and $V_i \geq V_j$. Let d denote the number of non-dominant solutions. If d exceeds N_e , N_e non-dominant solutions are randomly selected for removal. If d is smaller than N_e , we will randomly remove $(N_e - d)$ dominant solutions as well as d non-dominant solutions from the pool. Steps 2, 3, and 4 together define the evolutionary process that updates the population pool of solutions toward the Pareto front.

Step 5: repeat Repeat steps 2 to 4 to generate another new pool. Stop when m successive previously generated pools are received where the number of dominated Pareto solutions does not change or the total number of generation exceed G_{\max} (the maximum number of generations).

After steps 1 to 5 are implemented, the dominant building solutions in the final pool consist of solutions that approximate the Pareto front for the best building directions on the unit sphere.

Table 2 Pareto solution of motor mount model

Direction number	Building direction coordinates on unit sphere			Part height (in.)	Ranking on part height	Volume deviation (in. ³)	Ranking on volume deviation
	x	y	z				
1	0.00437	-0.3604	0.93279	0.07803	1	0.04193	10
2	-0.01218	0.3228	-0.94639	0.07922	2	0.04146	9
3	-0.01243	0.2756	-0.96119	0.07982	3	0.04074	8
4	-0.01363	-0.26703	0.96359	0.08004	4	0.0406	7
5	-0.00912	-0.21939	0.97559	0.08122	5	0.03975	6
6	-0.00741	-0.17127	0.9852	0.08243	6	0.03881	5
7	-0.00555	-0.12294	0.9924	0.08343	7	0.037778	4
8	-0.00134	0.07993	-0.9968	0.08397	8	0.03679	3
9	-0.00128	-0.07478	0.9972	0.08405	9	0.03667	2
10	0	0	1	0.08500	10	0.03488	1

2.4 Optimization criteria

In this paper, the authors chose two optimization criteria- part height and volume deviation—to illustrate the proposed multi-sphere model. Although the present work optimizes two criteria, other criteria can be added as illustrated by Fig. 4.

2.4.1 Part height

Part height describes the distance of material deposition along the building direction, and is a parameter indicating the dimensional limit of a rapid prototyping machine on part size that they can produce. As the building direction changes, part height will change accordingly. Given the geometry is in STL format in rapid prototyping processes, part height can be calculated by projecting the vertexes of each triangular facet comprising the STL model onto each candidate building direction. The distance between the two extreme projection points, highest level and lowest level, along the building direction is the part height. Figure 6 shows one building direction on the discretized unit sphere, and the part height calculated through projecting the vertexes of the STL model on the building direction. The same process will be repeated for each discretized direction on the unit sphere, and the calculated part height will be assigned to the corresponding discretized point on the unit sphere. Upon completion of this process, the first directional space for optimization is obtained.

2.4.2 Volume deviation

The second optimization criterion is TVD. Due to the staircase nature of rapid prototyping processes, volume deviation is inevitable between a tessellated model and the actual built volume through layer-stacking. Volume deviation is dependent on a number of parameters including layer thickness, building direction, tessellation granularity, etc. However,

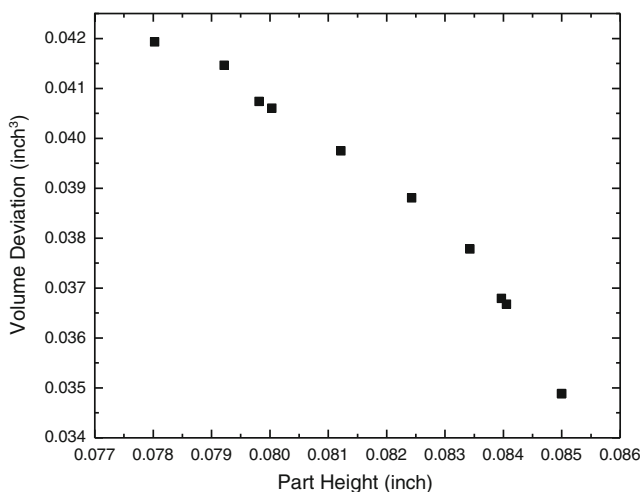


Fig. 11 Pareto front of part 1

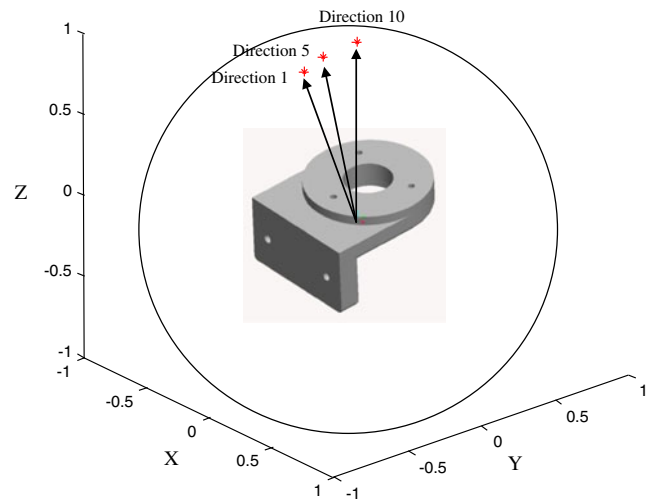


Fig. 12 Selected building directions of part 1 on a unit sphere

surface model tessellation and STL model-slicing are prior steps before searching for a building direction for an RP operation. Therefore, layer thickness and tessellation granularity are assumed to be given and remain unchanged during optimizing the building direction in this paper. Depending on the specific RP processes, the stair edges may be rounded to some extent [2]. However in this paper, we assume that the each layer has sharp edges in order to give a general way to evaluate the volumetric error, and thus the volumetric deviation is defined as theoretical volume deviation.

Since triangular facets are the basic elements comprising an STL model, the theoretical volumetric deviation is then calculated for each triangular facet along the building direction. Each stair consists of a stair space bounded by two perpendicular stair surfaces, the intersection of which is the internal edge of the stair (Fig. 7). The other two convex edges are

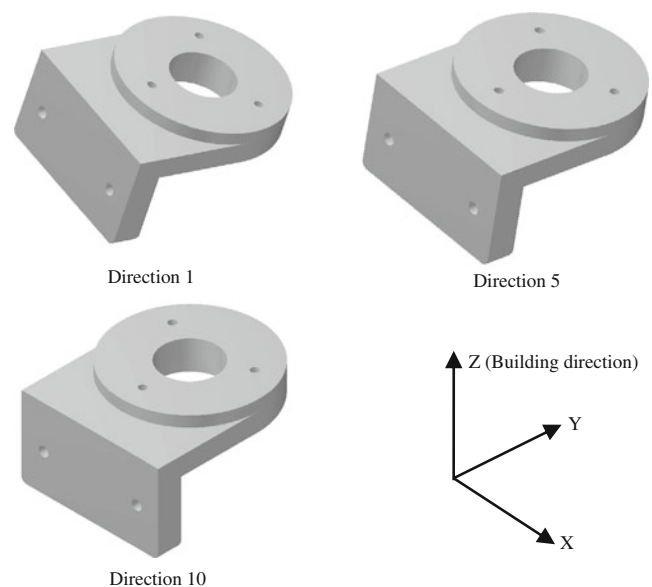


Fig. 13 Selected building directions of part 1

Table 3 Pareto solution of motor model

Direction number	Building direction coordinates on unit sphere			Part height (in.)	Ranking on part height	Volume deviation (1.0×10^{-3} in. ³)	Ranking on volume deviation
	<i>x</i>	<i>y</i>	<i>z</i>				
1	-0.01296	0.99989	0.00167	6.8909	1	192.573	14
2	0.00123	-0.99954	-0.03034	7.01014	2	191.752	12
3	-0.00761	0.92829	-0.37179	7.86594	3	191.752	12
4	0.01649	-0.85572	0.51717	8.11116	4	188.797	11
5	-0.01811	0.80436	-0.59386	8.15815	5	187.161	10
6	0.00482	-0.82127	0.57052	8.16261	6	186.78	9
7	0.02456	-0.78279	0.62187	8.16313	7	187.662	8
8	-0.02224	0.7648	-0.64388	8.22139	8	185.555	7
9	0.03038	-0.74124	0.67056	8.37718	9	185.095	6
10	-0.03148	0.72195	-0.69123	8.45533	10	184.149	5
11	0.0116	-0.65069	0.75925	8.69388	11	177.952	4
12	0.0254	-0.0055	0.79927	8.78951	12	176.671	3
13	0	0	1	10.1252	13	155.075	2
14	0.99986	0.00827	-0.01434	12.2516	14	96.6128	1

called external edges. There are three cases for the location of a triangular facet, depending on their vertices' locations.

1. Three vertices are in three different stair spaces.
2. Two vertices are in one stair space with the third vertex in a different stair space.
3. Three vertices are all in one stair space.

Figure 8 illustrates case 1, where three vertices of a triangular facet *ABC* are in three different stair spaces. Vertices *A*, *B* and *C* are projected onto the corresponding internal edge as *A'*, *B'*, and *C'*, respectively. The sub-volume deviation in the stair where vertex *A* (the lowest vertex of the triangular facet along the building direction) resides is a pyramid denoted as pyramid type 1 (*P*₁). The sub-volume deviation in the stair where vertex *B* (the highest vertex of the triangular facet along the building direction) resides is a pyramid denoted as pyramid type 4 (*P*₄). The sub-volume deviation in the stair where vertex *C* (the vertex between *A* and *B* along the building direction) resides is the summation of a wedge denoted as wedge type 2 (*W*₂) and two pyramids denoted as pyramid type 3 (*P*₃) and pyramid type 4 (*P*₄), respectively. It can be seen that *P*₃ and *P*₄ are sharing the base in Fig. 8, where the apex of *P*₃ is on the internal edge while the apex of *P*₄ is vertex *C*. The last type of sub-volume is denoted as wedge type 1 (*W*₁) which is bounded by two external edges. It should be noted that for this case there is one sub-volume *P*₁, *P*₂, *P*₃, *P*₄ and *W*₂ when calculating volume deviation for triangular facet *ABC*. However, there may be one or more than one sub-volume *W*₁, depending on the layer thickness. Therefore the theoretical volume deviation for this case is summarized as:

$$TVD = P_1 + P_2 + P_3 + P_4 + W_2 + \Sigma W_1$$

Figure 9 illustrates case 2, where two vertices are in one stair space with the third vertex in a different stair space. Vertices *A*, *B* and *C* are projected onto the corresponding internal edges as *A'*, *B'*, and *C'* respectively. *B* and *C* are in the same stair case. The sub-volume in the stair where vertices *B* and *C* reside is the summation of two pyramids (pyramid *B-B'EFC'* and pyramid *C-C'BF*) denoted as pyramid type 5 (*P*₅) and pyramid type 6 (*P*₆), respectively. The sub-volume deviation in the stair where vertex *A* (the lowest vertex of the triangular facet along the building direction) resides is of type *P*₁ as in case 1. Depending on the layer

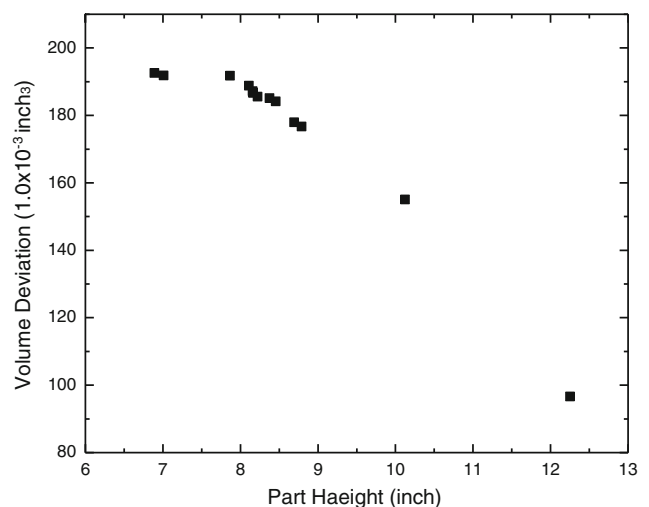


Fig. 14 Pareto front of part 2

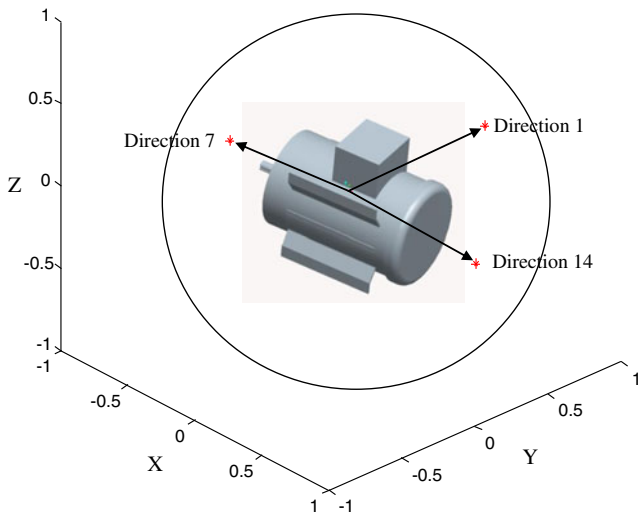


Fig. 15 Selected building directions of part 2 on a unit sphere

thickness, there may be one or more than one wedge of type W_1 . Therefore the theoretical volume deviation for this case is summarized as

$$TVD = P_1 + P_5 + P_6 + \Sigma W_1$$

Figure 10 illustrates case 3, where three vertices A, B and C are all in one stair space, and they project onto the internal edge as A', B', and C' respectively. Figure 10 also shows the adjacent facets around triangular facet ABC, the volume deviation of which can be calculated using cases 1 and 2 introduced above. The volume deviation of triangular facet ABC is described by the red polyhedron in Fig. 10 and can be decomposed into three pyramids B'-ABC, A'-AB'C, and C'-

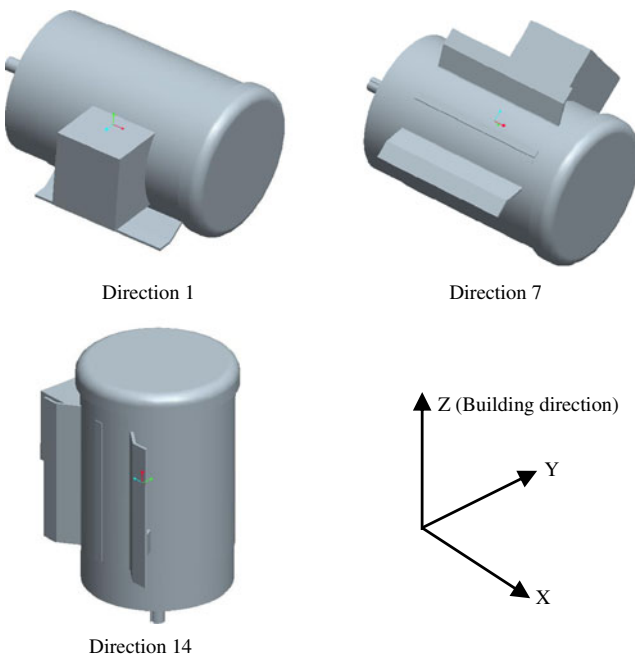


Fig. 16 Selected building directions of part 2

CAA', which are denoted by pyramid type 7 (P_7), pyramid type 8 (P_8) and pyramid type 9 (P_9), respectively. Therefore the theoretical volume deviation for this case is summarized as

$$TVD = P_7 + P_8 + P_9$$

This section illustrates the calculation of theoretical volume deviation based on geometrical volume decomposition. These three cases can be used to compute the theoretical volume deviation of each facet along a building direction candidate. The summation of theoretical volume deviation of all facets along this direction will be assigned to the corresponding point on the discretized unit sphere. The same process will be repeated for each discretized direction on the unit sphere. Upon completion of this process, the second directional space for optimization is obtained. As the user adds more optimization objectives, the similar process will assign objective function values to each individual discretized unit sphere. With n criteria selected, n discretized unit spheres with assigned objective function values collectively become the global optimization space.

3 Implementation

The GA-based Pareto algorithm is implemented in C++ programming language. Three geometrical models are tested for the Pareto front. Their geometries and the number of facets comprising the STL models are shown in Table 1. Included in the C++ program are unit sphere discretion, optimization criteria evaluation and genetic algorithm implementation.

To test the three example models, a unit sphere is uniformly discretized into 10,000 points ($N=10,000$) using Saff and Kuijlaars' algorithm [21]. An initial pool of $N_p=15$ directions are randomly picked from the discretized unit sphere for the first generation. In the next generation, $N_e=15$ new building directions are generated using both crossover and mating operations with half of them ($p=0.5$) produced by crossover and the other half by mutation, respectively. Then $N_p=15$ out of $N_p+N_e=30$ best building directions are chosen to form the pool for the next generation. A maximum number of generations $G_{max}=1,000$ are performed unless the pool stays the same for a number of $m=50$ generations.

The first model is a motor mount [37] that has 880 triangular facets. Table 2 shows the solution of the motor mount model, including building direction coordinates on the unit sphere, part height, volume deviation as well as the ranking of each direction in terms of part height and volume deviation. The columns on part height and volume deviation in Table 2 form the Pareto front for the two optimization criteria of the best building directions, as shown in Fig. 11. Figure 12 shows directions 1, 5, and 10 of part 1 on the unit sphere, and Fig. 13 shows the part model as directions 1, 5, and 10 are oriented to align with the Z-axis of a rapid prototyping machine.

Table 4 Pareto solution of bladed propeller model

Direction number	Building direction coordinates on unit sphere			Part height (in.)	Ranking on part height	Volume deviation (1.0×10^{-3} in. ³)	Ranking on volume deviation
	x	y	z				
1	0	1	0	2.73685	1	112.229	15
2	0.08504	-0.96549	0.24616	3.45003	2	110.104	14
3	-0.11708	0.90259	-0.41428	4.5658	3	105.483	13
4	-0.13023	0.85946	-0.49433	5.3232	4	101.987	12
5	0.33423	-0.82723	-0.45163	5.86507	5	99.3061	11
6	-0.49356	0.78185	0.38092	6.41076	6	95.829	10
7	0.34353	-0.71937	-0.60374	7.2298	7	90.5541	9
8	-0.48249	0.66927	-0.56504	7.6321	8	89.6604	8
9	0.28487	-0.61274	-0.73716	8.1063	9	81.6389	7
10	0.29081	-0.53306	-0.79453	8.68768	10	75.7705	6
11	-0.80715	0.4453	0.38759	9.16469	11	69.4979	5
12	0.78089	0.34662	0.51968	9.55699	12	64.6302	4
13	-0.90156	0.18395	0.39159	9.9761	13	59.3527	3
14	-0.25999	-0.02413	0.96531	10.4135	14	56.62	2
15	-0.6383	-0.13879	0.75717	10.9967	15	54.6168	1

The second model is a motor that has 840 triangular facets. Table 3 shows the solution of the motor model, including building direction coordinates on the unit sphere, part height, volume deviation as well as the ranking of each direction in terms of part height and volume deviation. The columns on part height and volume deviation in Table 3 form the Pareto front for the two optimization criteria of the best building directions, as shown in Fig. 14. Figure 15 shows directions 1, 7, and 14 of part 2 on the unit sphere, and Fig. 16 shows the part model as directions 1, 7, and 14 are oriented to align with the Z-axis of a rapid prototyping machine. It can be seen that directions 13 and 14 are far from the other directions on the Pareto front of part 2.

The third model is a bladed propeller [37] that has 1,052 triangular facets. Table 4 shows the solution of the bladed propeller model, including building direction coordinates on the unit sphere, part height, volume deviation as well as the ranking of each direction in terms of part height and volume deviation. The columns on part height and volume deviation in Table 4 form the Pareto front for the two optimization criteria of the best building directions, as shown in Fig. 17. Figure 18 shows directions 1, 8, and 15 of part 3 on the unit sphere, and Fig. 19 shows the part model as directions 1, 8, and 15 are oriented to align with the Z-axis of a rapid prototyping machine.

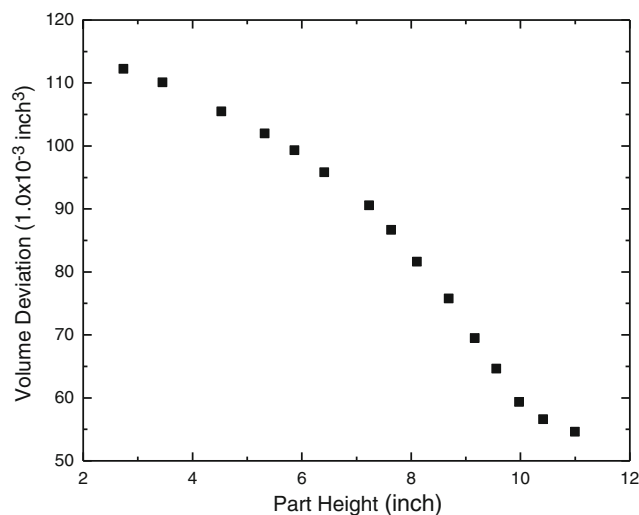


Fig. 17 Pareto front of part 3

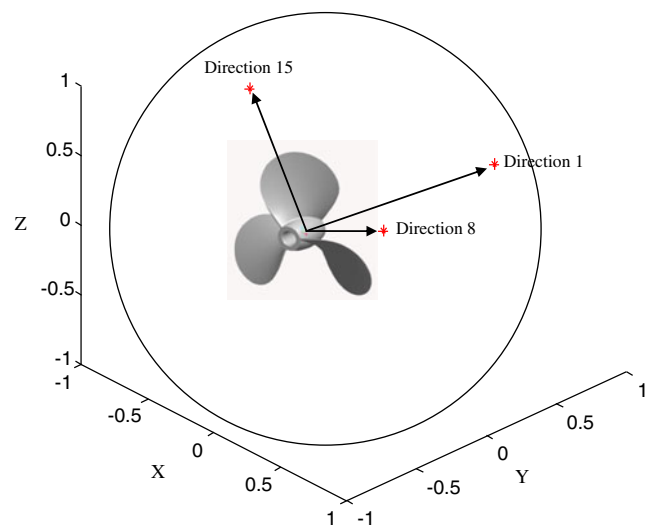


Fig. 18 Selected building directions of part 3 on a unit sphere

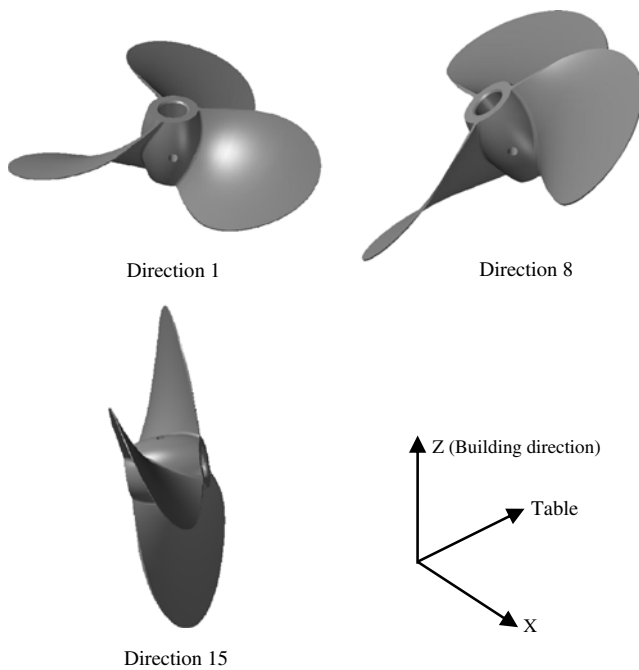


Fig. 19 Selected building directions of part 3

4 Conclusion

This paper presents a genetic algorithm-based Pareto optimization of building direction for rapid prototyping. Two objectives that are simultaneously optimized are part height and volume deviation. For each objective, a unit sphere is uniformly discretized as the searching space. This step makes it possible to massively compute and evaluate optimization objectives in the directional space. In order to evaluate the volumetric error in a general way, the concept of TVD is calculated along each building direction based on volume decomposition. Pareto front is also computed to show the competing effect from these two criteria. Although currently only two criteria are evaluated, more criterion can be added into the optimization model.

Like dimensional tolerance requirements on machined parts depend on the specific geometric features, surface quality requirements are not uniform on rapid prototyped parts. This suggests that Pareto front needs to treat different surfaces separately. Therefore as our future work, the Pareto-based optimization model will expand to regional analysis on the CAD model.

References

- Kamrani AK, Nasr EA (2005) Rapid prototyping theory and practice. Springer, New York
- Byun HS, Lee KH (2006) Determination of the optimal build direction for different rapid prototyping processes using multicriterion decision making. *Robotics and Computer-Integrated Manufacturing* 22(1):69–80
- Ahn D, Kim H, Lee S (2007) Fabrication direction optimization to minimize post-machining in layered manufacturing. *Int J Mach Tool Manuf* 47(3–4):593–606
- Giannatsis J, Dedoussis V (2007) Decision support tool for selecting fabrication parameters in stereolithography. *Int J Adv Manuf Technol* 33(7–8):706–718
- Canellidis V, Giannatsis J, Dedoussis V (2009) Genetic-algorithm-based multi-objective optimization of the build orientation in stereolithography. *Int J Adv Manuf Technol* 45(7–8): 714–730
- Nikhil P, Kalyanmoy D (2011) Multi-objective optimization and multi-criteria decision making in SLS using evolutionary approaches. *Rapid Prototyping J* 17(6):458–478
- Rattanawong W, Masood SH, Iovenitti P (2001) A volumetric approach to part-build orientations in rapid prototyping. *J Mater Process Technol* 119(1–3):348–353
- Masood SH, Rattanawong W (2002) A generic part orientation system based on volumetric error in rapid prototyping. *Int J Adv Manuf Technol* 19(3):209–216
- Kumar C, Choudhury AR (2005) Volume deviation in direct slicing. *Rapid Prototyping J* 11(3):174–184
- Zhang J, Li Y (2012) A unit sphere discretization and search approach to optimize building direction with minimized volumetric error for rapid prototyping. *Int J of Adv Manuf Technol* (accepted). doi:10.1007/s00170-012-4518-0
- Hur S-M, Choi K-H, Lee S-H, Chang P-K (2001) Determination of fabricating orientation and packing in SLS process. *J Mater Process Technol* 112(2–3):236–243
- Gogate AS, Pande SS (2008) Intelligent layout planning for rapid prototyping. *Int J Prod Res* 46(20):5607–5631
- Ancau M, Caizar C (2010) The computation of Pareto-optimal set in multicriterial optimization of rapid prototyping processes. *Comput Ind Eng* 58(4):696–708
- Chan CK, Tan ST (2004) Putting objects into a cylindrical/rectangular bounded volume. *Computer Aided Design* 36(12): 1189–1204
- Allen S, Dutta D (1995) Determination and evaluation of support structures in layered manufacturing. *J of Design and Manuf* 5(3): 153–162
- Thompson DC and Crawford R H (1995) Optimizing part quality with orientation. *Proceedings of the 1995 Solid Freeform Fabrication Symposium, Austin, Texas*
- Kim JY, Lee K, Park JC, Jung YH (1998) Efficient calculation of trapped volumes in the layered manufacturing process. *Int J Adv Manuf Technol* 14(12):882–888
- Cheng W, Fuh JYH, Nee AYC, Wong YS, Loh HT, Miyazawa T (1995) Multi-objective optimization of part-building orientation in stereolithography. *Rapid Prototyping J* 1(4):12–23
- Hur J, Lee K (1998) The development of a CAD environment to determine the preferred build-up direction for layered manufacturing. *Int J Adv Manuf Technol* 14(4):247–254
- Pandey PM, Thrimurthulu K, Venkata NR (2004) Optimal part deposition orientation in FDM by using a multicriteria genetic algorithm. *Int J Prod Res* 42(19):4069–4089
- Saff EB, Kuijlaars ABJ (1997) Distributing many points on a sphere. *Math Intell* 19(1):5–11
- Chen LL, Woo TC (1992) Computational geometry on the sphere with application to automated machining. *ASME J of Mechanical Design* 114:288–295
- Chen LL, Chou SY, Woo TC (1993) Parting directions for mould and die design. *Computer-Aided Design* 25(12):762–768
- Spitz SN, Spyridi AJ, Requicha AAG (1999) Accessibility analysis for planning of dimensional inspection with coordinate measuring machines. *IEEE Trans Robot Autom* 15(4):714–727
- Yang ZY, Chen YH, Sze WS (2001) Determining build orientation for layer-based machining. *Int J Adv Manuf Technol* 18:313–322

26. Dhaliwal S, Gupta SK, Huang J, Priyadarshi A (2003) Algorithms for computing global accessibility cones. *ASME J of Computing and Inf Sci in Eng* 3(3):200–209
27. Zitzler E, Deb K, Thiele L (2000) Comparison of multi-objective evolutionary algorithms: empirical results. *Evol Comput* 8(2):173–195
28. Horn J, Nafpliotis N, Goldberg DE (1994) A niched Pareto genetic algorithm for multiobjective optimization. In: *Proceedings of the first IEEE conference on evolutionary computation*. IEEE world congress on computational intelligence, 27–29 June, 1994. Orlando, FL, USA:IEEE; 1994
29. Hajela P, Lin C-y (1992) Genetic search strategies in multicriterion optimal design. *Struct Optimization* 4(2):99–107
30. Murata T, Ishibuchi H (1995) MOGA: multi-objective genetic algorithms. In: *Proceedings of the 1995 I.E. international conference on evolutionary computation*, 29 November–1 December, 1995. Perth, WA, Australia: IEEE; 1995
31. Holland JH (1975) *Adaptation in natural and artificial systems*. University of Michigan Press, Ann Arbor
32. Goldberg DE (1989) *Genetic algorithms in search*. Addison-Wesley, Optimization and Machine Learning
33. Mitchell M (1996) *An introduction to genetic algorithms*. MIT Press, Cambridge
34. Schmitt LM (2001) *Theory of genetic algorithms*. *Theor Comput Sci* 259(1–2):1–61
35. Steuer RE (1986) *Multiple criteria optimization: theory, computations, and application*. John Wiley & Sons, Inc., New York
36. Sawaragi Y, Nakayama H, Tanino T (1985) *Theory of multiobjective optimization* (vol. 176 of *Mathematics in Science and Engineering*). Academic Press, Orlando. ISBN 0-12-620370-9
37. Grab CAD (2012) <http://grabcad.com/>. Accessed 3 July 2012
38. Li Y, Frank MC (2012) Computing axes of rotation for setup planning using visibility of polyhedral computer-aided design models. *ASME J of Manuf Sciand Eng* 134, p. 041005(1–10)